Green Ammonia for Energy: Characteristics, Conversion Routes, and System Integration

Hafiz Ali Muhammad[a], Muhammad Tanveer Ahmed Ranjah[b], Young Duk Lee[c]*

[a] *Korea Institute of Energy Technology (KENTECH), Naju-si, Rep. of Korea, hafiz@kentech.ac.kr*
[b] *Korea Institute of Energy Technology (KENTECH), Naju-si, Rep. of Korea, tanvir@kentech.ac.kr*
[c] *Korea Institute of Energy Technology (KENTECH), Naju-si, Rep. of Korea, ydlee@kentech.ac.kr, CA*

Abstract:
Ammonia has emerged as a promising carbon-free energy carrier and hydrogen vector for deep decarbonization of the power and gas sectors, due to its favorable physicochemical properties and the availability of extensive production, transport, and storage infrastructure. This study compares key ammonia-to-power conversion pathways from energy and exergy perspectives. Two principal systems are analyzed: a hydrogen-fueled gas turbine combined cycle with an integrated ammonia cracker, and a solid oxide fuel cell operated ammonia. Partial heating supercritical carbon dioxide (sCO_2) and steam cycles serve as bottoming configurations for the gas turbine.
The hydrogen gas turbine and the fuel cell stack are the crucial blocks of the complete system; hence, their models are corroborated with the experimental results. The results showed ammonia-fueled fuel cell achieves a power density 42% that of hydrogen, demonstrating its viability as a fuel candidate. The combined cycle with supercritical carbon dioxide surpassed the fuel cell and combine cycle with steam system with a net power, energy and exergy efficiency of 2.90 MW, 44.1% and 41.5% respectively. The exergy analysis revels the loss of exergy is significant for all cases with a magnitude of 30.48%, 43.8% and 63.44% for fuel cell, steam-gas turbine combined cycle and supercritical carbon dioxide combined cycle, respectively and any improvement measure should focus on recovering this exergy loss. This study provides critical insights into ammonia as a fuel, compares the performance of representative technologies and systematically identifies the source or irreversibility to foster an improved design. The current study quantifies the irreversibility and establishes a foundation for future optimization using advanced exergy methods by categorizing the avoidable and unavoidable parts of the exergy destruction.

Keywords:
Ammonia, Fuel characteristics, Utilization, Combined cycle, Electrochemical, Comparative analysis.

1. Introduction

Ammonia (NH_3) is a multifaceted compound that serves as a cornerstone in diverse industrial, agricultural, and energy applications. Its versatile application spectrum includes fertilizer production, refrigeration, mining, pharmaceuticals, water treatment, and usage as hydrogen-carrier and carbon-free fuel positioning it at the nexus of sustainability and innovation [1]. As a carbon-free energy carrier, NH_3 holds immense promise for reducing global carbon footprints while enabling energy storage and transport at scale. Its potential use in combustion engines, electrochemical conversion systems, and as a working fluid in advanced power cycles heralds a transformative shift in the energy generation paradigm.

While hydrogen (H_2) emerges as a catalyst for a carbon-free economy, it faces challenges concerning storage and distribution, hindering its widespread application [2]. Conversely, NH_3 possesses a high energy density (7.1 MJ/L) and established transportation network, presenting remarkable flexibility. NH_3 benefits from cost efficiency, established infrastructure and safety measures, as well production pathways compatible with renewables sources. These attributes position NH_3 as a practical contender for the next-generation energy transportation, storage, and power generation systems. Additionally, NH_3 offers innovative solutions to sustainability challenges within the energy industry. Several countries have begun to incorporate NH_3 as a low-carbon fuel into their future energy policies. Notably, the U.S. House of Representatives classified NH3 as a “low-carbon fuel” in January 2020. The UK's Royal Society also released a policy with a title of “NH3: Zero-Carbon Fertilizer, Fuel, and Energy Store”, which provides valuable information and analysis to support the development of regulatory policies regarding NH3's utilization within the clean energy technology portfolio [3].

NH_3 was initially seen as the carrier of H_2 but recently the trend has been shifted to directly used NH_3 for power generation. The NH_3 can suffice as electric power generation vector as well as a fuel for combustion engines making it a viable candidate for decarbonization of energy and transportation sector [4]. Two primarily distinct pathways for NH_3 electrification are i) as a fuel or with NH_3 cracking in a gas turbine combined cycle (GTCC) and (ii) electrochemical conversion in a fuel cell [5]. For the former category, different researchers have studied and proposed carious alternatives to be retrofitted to the gas turbine applications. The co-firing of NH_3 and coal with 20 vol% has been demonstrated under commercial conditions [6]. For natural gas engines, combustors capable of handling various fuel mixtures with NH_3 has also been investigated. In addition to cofiring, the decomposed NH_3 can be used in GTCC and the exhaust gas heat can be integrated with the NH_3 cracking reactor. This aspect has been studies from the techno-economic perspective. Jeong and Kim [7] analyzed a GTCC configuration co-fired with partially cracked ammonia and natural gas and reported an efficiency penalty of 0.27%. From the economic perspective, Cesaro et al. [8] compared the levelized cost of electricity for NH_3, partially cracked NH_3 and H_2 and found out that employing NH_3 cracking results in highest levelized cost. Among the fuel cell, the high temperature solid oxide fuel cell offers superior performance and hence is considered in this study. The comparative study of NH_3 in internal combustion engines and fuel cell concluded that fuel cell operating with combined power, heating and cooling is the most efficient system for NH_3 utilization [9].

The previous studies focus on one of end-use modality that can run on NH_3 or assessing the combustion characteristics but lacks in system level comparative assessment of different technologies. The study sets out to thoroughly investigate the NH3 as fuel, its characteristics and its electrification from an energy and exergy perspective. The NH_3 characteristics and production routes are discussed. Distinctly, the comparison of the various fuels in a fuel cell operation in terms of power density are reported. For a rigorous analysis, the electrification of NH_3 in a gas turbine application with sCO2 and steam bottoming cycles well as fuel cell is investigated. For the gas turbine, KAWASKAI M1A-17 [10] which has already been operated on 100% H_2 is selected and is integrated with NH_3 pre-cracking to operate it with NH_3 fuel. In a gas turbine combined cycle (GTCC) power plant, NH_3 cracking can be thermally integrated with the exhaust gas [11] to provide the heat for the reaction and is adopted in this study. The fuel cell system is design with burner and fuel and air preheaters, and its operating strategy is devised and discussed. The heart of the combine system and the fuel cell system is M1A-17 turbine and stack whose designs are validated against the experimental results. The whole modelling is done in Ebsilon environment [12], which is a well-known commercial software for power generation system analysis. The system is comprehensively analysed from the perspective of the first and second law of thermodynamics and the performance of each system is reported in terms of power, first and second law efficiency and the destruction of exergy. Finally, the exergy analysis was done to get the insights of each system and identify the losses.

2. Production and Characteristics

The NH_3 production processes are studied vastly and summarized extensively in the literature. NH_3 production technologies can be broadly classified into three generations [1]. Gen 1 corresponds to the conventional Haber–Bosch (H-B) process upgraded with carbon capture and storage (CCS), enabling partial decarbonization in the near term. Over the next decade, deployment of Gen 1 technologies is expected to expand owing to its technical maturity and the need to meet the growing energy demand. Gen 2 retains the H-B synthesis route but replaces fossil-derived hydrogen with green hydrogen produced via renewable-powered water electrolysis. This pathway is projected to reach commercial readiness (CRI ≈ 3) around 2030, after which its deployment will grow rapidly, gradually displacing both current and Gen 1 processes. Gen 2 can produce green NH_3 only if the supplied H_2 is produced using renewable driven water electrolysis. Fully electrochemical, renewable-powered Gen 3 NH_3 synthesis with direct-electro chemical reduction of N_2 process are expected to reach initial commercial readiness (CRI 1) toward the end of this decade, however, there is doubt about the Gen 3 technology to become the preferred industrial choice, possibly due to the reliance of Gen 1 and 2 on the mature, industrially proven H-B and water electrolysis processes. Figure 1 puts into perspective the intrinsic fuel characteristics of NH_3 compared to other fuels. The LHV of NH3 is 41% of the liquefied gas but cost of NH3, developed infrastructure and its compatibility with different carbon-intensive processes make it the center of deep-decarbonization and H_2 economy.

3. Systems description and modelling

The representative routes of converting NH_3 into electricity are GTCC and fuel cell system which are both considered and analyzed in this study. The gas turbine was M1A-17 and is integrated with its operational parameters given in the Table 1. The conditions given are taken from the catalogue while some are taken as the author's hypothesis. The fuel inlet is pure H_2 which is mixed with the incoming air in the combustion chamber. The incoming air is branched in two streams; one serves as the dilution air and the other is utilized during the combustion. The burned gases reach high temperature and are then fed to the gas turbine. In the

gas turbine analysis, the exhaust gas composition, temperature and flow rate are calculated and compared. To operate it with the NH_3 fuel, the turbine was modified to have thermal cracker at the fuel inlet and integration of exhaust gases from the turbine out with the NH_3 cracking as shown in Figure 2.

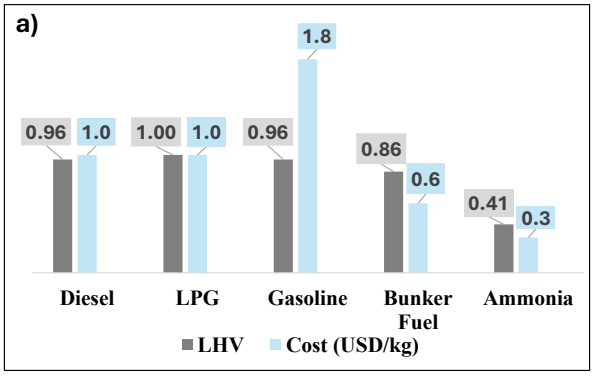

Figure 1. *NH_3 characteristics Normalized with respect to liquefied petroleum gas (LPG: 12.6 kWh/kg and 1 $/kg) [9].*

Table 1. *M1A-17 turbine specifications [10].*

Parameter	*Values*
Inlet T & P	15°C and 1.01 bar
Isentropic efficiency of compressor	0.80 (Assumed)
Primary air (at nozzle) $Air/Air_{Stoichiometric}$	1.4
Dilution air (at liner)	Calculated based on exhaust gas temperature
Pressure ratio	10.5:1
Fuel consumption (using LHV)	0.057 kg/s
Turbine efficiency	0.88 (assumed)
Pressure drops	Neglected
Exhaust stream temp	528°C

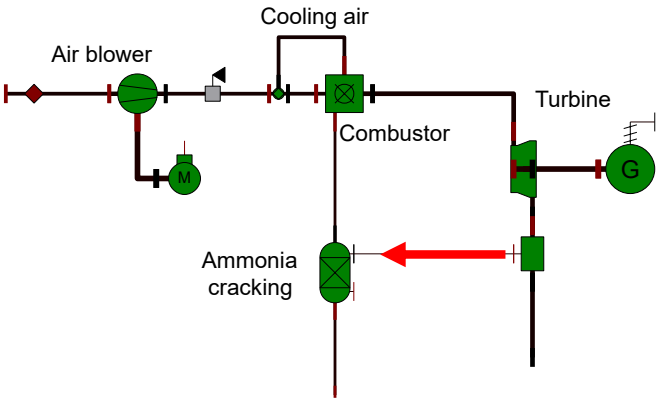

Figure 2. *Gas turbine model with NH_3 cracking.*

After expansion in the gas turbine, the low pressure and high temperature gases are then fed to a high temperature heat source (HTHS) for the bottoming cycle. One bottoming cycle is the partial heating cycle as shown in Figure 3(a) which employs two heat sources, one recuperator, one turbine, one compressor and one cooler. The heat recovery from the flue gas happens in two recovery heat exchangers, i.e. low temperature heat source and high temperature heat source. The splitting of heat recovery increases the recovery rate which is the primary characteristic of a partial heating cycle. The configuration of the steam cycle is shown in Figure 3(b) and was adopted from [13] with one reheater, deaerator and expansion occurred in four stages.

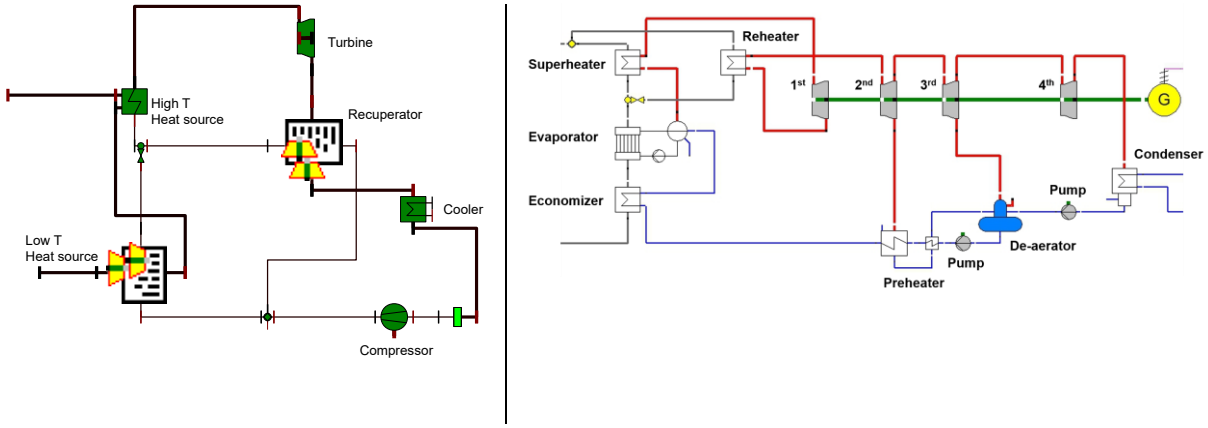

Figure 3. Bottoming cycle**,** Partial heating sCO_2 cycle (left) and steam cycle (right).

Finally, the balance of plant design for the fuel cell system is shown in Figure 4.The design employed fuel and air preheaters and combustion. The anode and cathode off gases are mixed and fed to a combustor. After the combustion, the flue gasses are split and directed to the air and fuel preheater where they are employed to preheat the fuel and air to the desired stack inlet conditions.

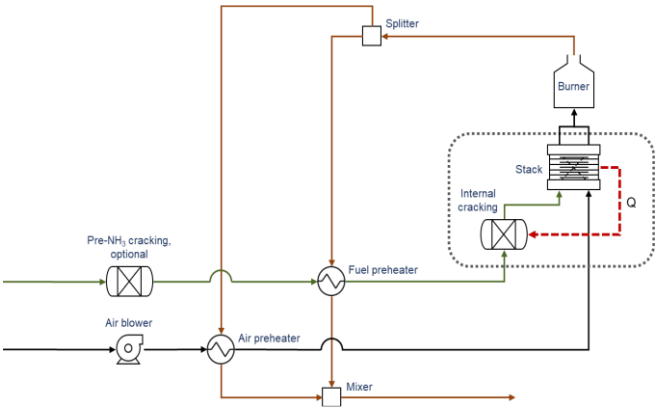

Figure 4. *Fuel cell system.*

The turbomachinery is modeled using isentropic efficiency while the heat exchangers are modelled based on the pinch point (PP). Pertaining to the sCO_2 cycle, the evolution of PP during the heat transfer is vital and thus carefully addressed using a user-define model for the recuperator. The low- and high-pressure levels of the cycle are selected as 200 and 85 bar, respectively. The high pressure is selected as a commonly accepted pressure level in the scope of sCO_2 [14]. The low-pressure level is selected so that the system remains in the supercritical state. The turbine inlet temperature (TIT) was fixed at 375°C and the cooling temperature was 30°C. The compressor exhibits low efficiency in the supercritical region due to the operation of compressor near the critical point thus the compressor efficiency is taken as 0.70. For the steam the high-level pressure of 120 bar is selected so that the at the outlet of final stage turbine, the steam quality is greater than 90% and the back pressure was selected as 1 bar. For the fuel cell system, the fuel input is same as for the combined cycle. The stack size was calculated to achieve the fuel utilization of 0.75 across the stack. The boundary conditions used for the complete modelling are summarized in Table 2.

3.1. Ammonia fuel cell modelling

Table 2*. Boundary conditions for the analysis.*

Parameters	sCO_2 cycle	Steam cycle	Fuel cell
Turbine inlet pressure (TIP)	200 bar	120 bar	N/A

Turbine inlet temperature (TIT)	375°C	382°C	N/A
Turbine outlet pressure (TOP)	85 bar	1 bar	N/A
Compressor inlet temp	30°C	N/A	N/A
Compressor efficiency	0.70	N/A	N/A
Turbine efficiency	0.88		N/A
Heat exchanger pinch points	15°C		N/A
Ammonia cracking reactor temperature	480°C	480°C	
Flue gas conditions	From M1A17 turbine with Ammonia cracking		N/A
Stack temperature	N/A		800°C
Fuel utilization			0.75

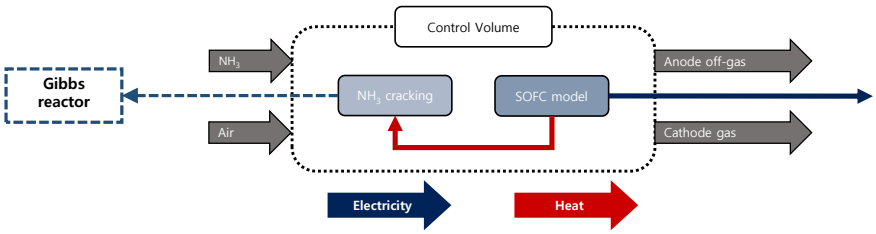

Figure 5. *Ammonia fuel cell modeling.*

The SOFC is the critical component of the whole chain, and the modelling details are given in various articles [15,16]. The chemical reactions occurring in particularly H_2 fueled SOFC are well understood and the cell potential are summarized in theTable 3. In a fuel cell V_{Actual} and $V_{Reversble}$ are actual and reversible voltages while V_{Ohmic}, V_{Conc}, and $V_{Activation}$ are ohmic, concentration and activation losses, respectively. The equations summarized in the table are those used for the H_2 fueled SOFC. This study adopted the similar procedure for the NH_3 fuelled SOFC with one exception as illustrated in the Figure 5. In the NH_3 fueled SOFC, ammonia cracking happens simultaneously with the electrochemical reaction, however, this study assumed that 100% NH_3 cracking happen in the initial phase, thus the NH3 cracking was simulated before the fuel cell using a Gibbs reactor. The heat required for the ammonia cracking was supplied from the fuel cell to reflect that the cracking and electrochemical reaction happens within the control volume.

3.2. Performance indicators

The analysis is done from the first law and the second law perspective. The net power of the combined cycle and the fuel cell system is given in Eq. (1) and (2) respectively.

$$W_{CombineCycle} = W_{Bottoming\ cycle} + W_{Gas\ turbine} \quad (1)$$

$$W_{Fuel\ cell\ system} = W_{Stack\ power} - W_{Air\ blower} \quad (2)$$

The bottoming cycle analyzed are steam and sCO2 cycle while the $W_{Gas\ turbine}$is the power generation from M1A-17 gas turbine with NH_3 cracking. For the fuel cell system, the net power is the stack power ($W_{Stack\ power}$) minus the power consumed by the air blower ($W_{Air\ blower}$). The first law efficiency of the whole system is defined based on the lower heating value of the fuel and is given by Eq. (3).

$$Energy\ efficiency = \frac{W_{CombineCycle}}{m_{Fuel} * LHV_{Fuel}} \quad (3)$$

The second law is employed to calculate the exergy balance and the exergy efficiency. The exergy of any stream (*Ex*) is the sum of physical (Ex_{Ph}) and chemical exergy (Ex_{Ch}) and is the function of its thermodynamic state and the reference environment. The *Ex*, Ex_{Ph} *and* Ex_{Ch} is given in the *Eq. (4-6)* where x_i and $e^{CH,standard}$are mole fraction and standard chemical exergy of a substance [17,18].

$$Ex = Ex_{Ph} + Ex_{Ch} \quad (4)$$

$$\mathrm{ex_{Ph}} = \mathrm{h} - \mathrm{h_o} - \mathrm{T_o}(\mathrm{s} - \mathrm{s_o}) \quad (5)$$

$$ex_{Ch} = \Sigma x_i * e^{CH,standard} + R * T_o \Sigma x_i \ln(x_i) \quad (6)$$

The exergy balance and the exergy efficiency of the component is given by Eq. (7) and (8).

$$Ex_F = Ex_P + Ex_D + Ex_L \quad (7)$$

$$Exergy\ efficiency = Ex_P / Ex_F \quad (8)$$

Where the Ex_P and Ex_F are the product and fuel exergy respectively and are described based on the purpose of the system. Ex_D and Ex_L are the exergy destruction and the loss of exergy respectively. For the overall system the exergy balance is given by Eq. (9).

$$Ex_{F,Total} = Ex_{P,Total} + \sum Ex_D + Ex_{L,Total} \quad (9)$$

Table 3. *Fuel cell modeling.*

Potential	*Equation*		*Comments*
Total voltage	$V_{Actual} = V_{Reversible} - V_{Ohmic} - V_{Activation} - V_{Conc}$	(A1)	
Reversible voltage	$V_{Nernst} = E^0 + \frac{R_g T_s}{2F} \ln\left(\frac{p_{H_2} \cdot {p_{O_2}}^{0.5}}{p_{H_2O}}\right)$ $E^0 = 1.2723 - 2.7645 \times 10^{-4} \times T_s$	(A2-A3)	Where R and F are gas and faraday constant, T is operating temperature, and P is partial pressures.
Ohmic losses	$\eta_{ohm} = \frac{\rho_{an}\delta_{an} + \rho_{ca}\delta_{ca} + \rho_{el}\delta_{el} + \rho_{Int}\delta_{int}}{A_{cell}}$		Where δ is thickness and i is current density.
Activation losses	$i = i_0 \left\{ exp\left(\beta \frac{n \cdot F \cdot \eta_{act}}{RT_s}\right) - exp\left[-(1-\beta)\frac{n \cdot F \cdot \eta_{act}}{RT_s}\right]\right\}$ $= 2i_0 \sinh\left(\frac{n \cdot F \cdot \eta_{act}}{2RT_s}\right)$	(A4)	Where k can be cathode or anode and i_o is limiting current. n is number of electrons.
Concentration losses	$\eta_{con,an} = -\frac{RT_s}{2F} \times \ln\left[\frac{1 - \left(\frac{RT_s}{2F}\right)\left(\frac{\delta_{an}}{D_{an,eff} p_{H_2,an}}\right) j}{1 + \left(\frac{RT_s}{2F}\right)\left(\frac{\delta_{an}}{D_{an,eff} p_{H_2O,an}}\right) j}\right]$ $\eta_{con,ca} = -\frac{RT_s}{4F} \times \ln\left[\frac{\left(\frac{P_{ca}}{\beta_{O_2}}\right) - \left(\frac{P_{ca}}{\beta_{O_2}} - p_{O_2}\right) \exp\left(\frac{RT_s}{4F}\right)\left(\frac{\beta_{ca}\delta_{ca}}{D_{ca,eff} P_{ca}}\right) j}{p_{O_2}}\right]$	(A5-A6)	$D_{H2o,Eff}$, $D_{K,Eff}$, and $D_{O,Eff}$ are effective, Knudsen and ordinary diffusion coefficient respectively. The pressure is in pascals. $r_{Particle}$is particle radius and M is molar mass.

4. Validation

The gas turbine results are summarized in Table 4. The Ebsilon model demonstrates reasonable accuracy in predicting performance. The relatively high calculated power output can be attributed to the assumption of negligible pressure losses. The burning characteristics and temperature are not reported so a direct comparison was not possible.

Table 4*. Performance comparison of gas turbine.*

Parameter	**M1A-17 catalogue**	**Calculated**
Power [MWe]	1.90	1.97
Exhaust gas temp [°C]	528	528
Exhaust gas flow [kg/s]	7.89	8.16

For the fuel cell system, the user defined model for the stack was corroborated with the experimental results and is shown in Figure 6. The model predictions are in good agreement with the experimental results except at the higher current density operation which is being further investigated.

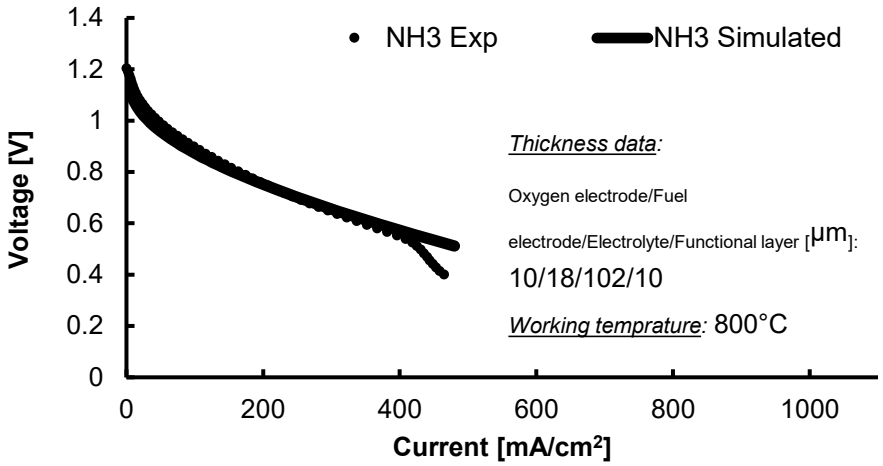

***Figure 6**. Validation of the fuel cell model.*

5. Results

The performance of the ammonia-fueled gas turbine and fuel cell was analyzed from both energy and exergy perspectives. The fuel cell used an electrolyte-supported design, and to evaluate the operation with different fuels, the same stack was simulated using H_2, reformed methane (CH_4), and NH_3. Figure 7 shows the comparison and as anticipated the direct fired H2 fuelled cell offers the best performances since there are no other species, thus the activation and concentration losses are minimum. The reformed CH_4 and NH3 offers similar performance. For a fixed operating temperature and voltage of 800° and 0.8 V, the power density for H2, NH3 and CH4 are 0.28, 0.12 and 0.15 W/m2, respectively. Although the LHV of NH_3 is only 16% that of H_2, its power density reaches 42.8% of the H_2 case, demonstrating that NH_3 is a promising fuel candidate for fuel cell operation as shown in the Figure 8.

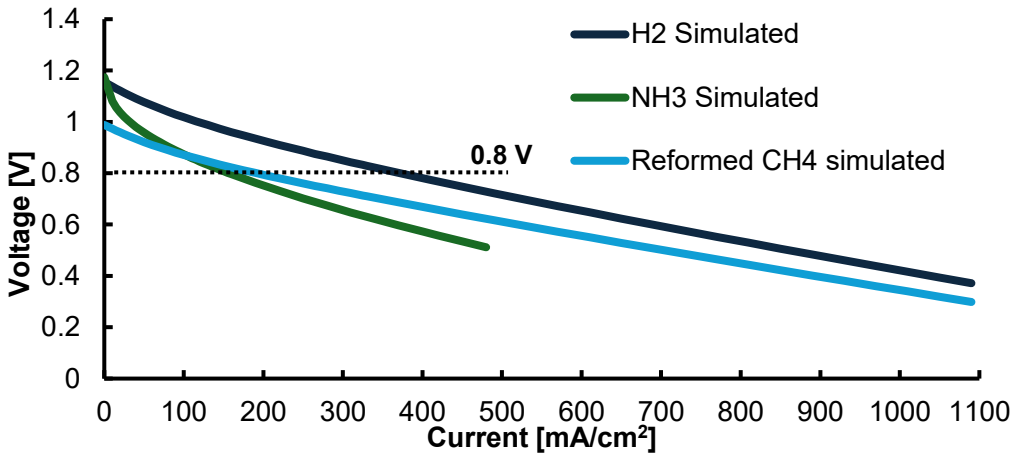

***Figure 7.** IV characteristics of different fuels.*

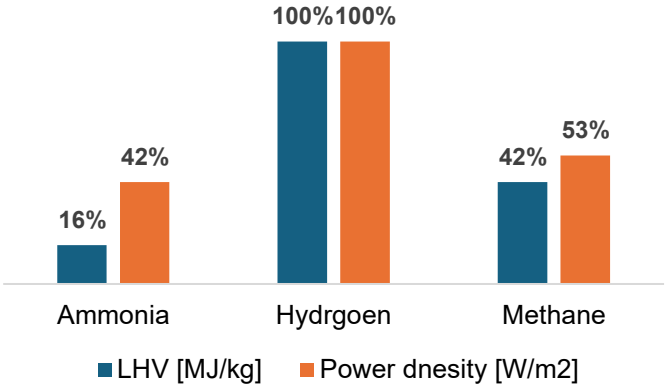

Figure 8. *Ammonia characteristics with respect to normal fuel for fuel cells Normalized with respect to H2, i.e. LHV of 120 MJ/kg power density of 0.28 W/m^2.*

5.1. Energy analysis

The power generation systems are analysed with a fixed fuel inlet of 6584.597 kW for all the cases. The net power generation by each system, i.e. combined cycle with steam, with sCO2 and fuel cell are 2.65, 2.90 and 2.87 MW respectively as shown in the Figure 9.

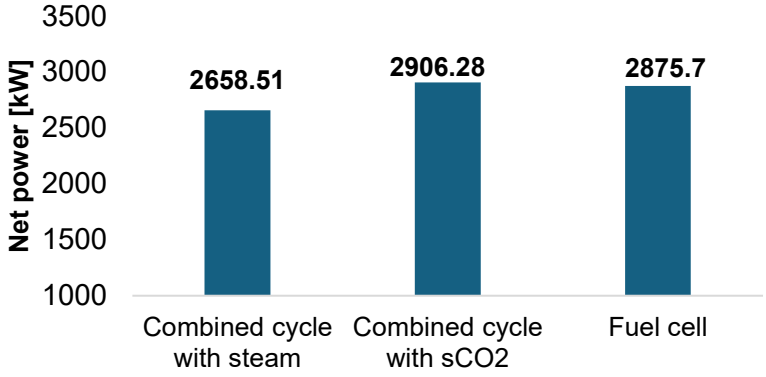

Figure 9. Net power generation [kW] by each system.

The energy and exergy efficiency of the systems are illustrated in the Figure 10. The sCO2 combined cycle surpassed the competitive system with a net power, energy and exergy efficiency of 2.90 MW, 44.1% and 41.5% respectively. The further elaboration is done using the exergy balance as discussed in the following section. However, the first law (energy) analysis is limited to assessing the extent of heat source utilization, whereas the exergy analysis offers deeper insight into system behavior and optimization by quantifying the irreversibility and losses within the process.

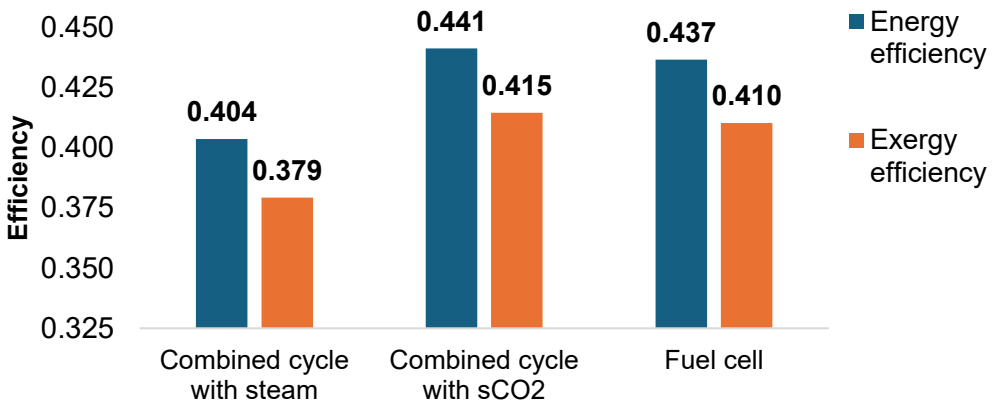

Figure 10. *System and exergy efficiency of each system.*

5.2. Exergy analysis

The exergy analysis is conducted by formulating the fuel and product exergy of each component in each system. The exergy balance for fuel cell, gas turbine with NH_3 cracking and the bottoming cycle are done and Table 5 shows the balance for the fuel cell while it is omitted for other components due to brevity. The system fuel exergy is same for the gas turbine and the fuel cell, since they are supplied with the same fuel flow and heating rate. Moreover, the sum of exergy at the tailpipe is the loss of exergy while the gas turbine has no losses of exergy, since the exhaust gas is used as a heat source for the topping cycle. In the power generation cycle, the fuel exergy of the cooler and the exhaust stream is the loss of the exergy to the environment. The sum of exergy destruction and loss for each system are given in the Figure 11, where the minimum destruction is in the fuel cell followed by sCO2 and steam combined cycle.

Table 5. *Exergy balance for the fuel cell.*

Component	*Fuel exergy [kW]*	*Product exergy [kW]*
Air blower	533.03	108.01
Air preheater	5913.87	4843.20
Fuel preheater	514.38	376.0
Fuel cell	5036.98	4050.45
Combustor	7962.97	7737.88
Exergy loss (Sum of exergy at fuel and air preheater out)	1247.71	
System	7124.12	2875.72

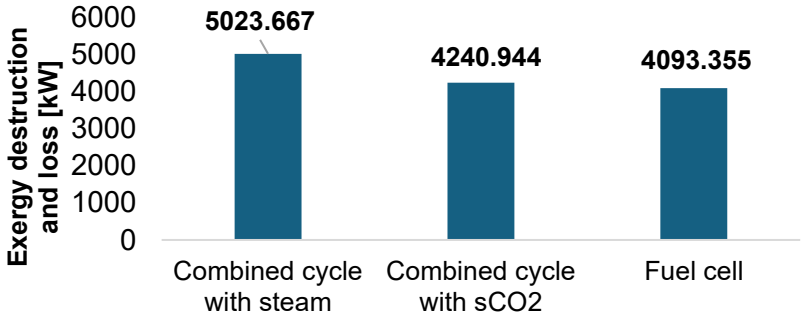

Figure 11. *Exergy destruction and loss [kW].*

The exergy balance was carried out to reveal the destruction and consequentially the improvement potential. The exergy destruction of each power generation system was summarized in the Figure 12. The exergy

destruction for the gas turbine with ammonia cracking, fuel cell, sCO_2 cycle, and steam cycle occurs in the following order: combustion > air blower > turbine > ammonia cracking; exergy loss > air preheater > fuel cell > air blower > combustor > fuel preheater; exhaust gas, exergy loss > cooler, exergy loss > low-temperature heat source > recuperator > turbine > compressor > high-temperature heat source; and exhasut gas loss>turbine > cooler, exergy loss > steam generator > superheater > reheater > feedwater preheater > deaerator, respectively. For the individual sub systems, the analysis reveals the maximum potential for improvement in gas turbine is at the combustor and the minimum potential is with the ammonia cracking reaction. The plausible reason is the combustion chamber is fed with the hydrogen and nitrogen fuel mixture which could increase the irreversibility during combustion. The Ammonia cracking reaction is simulated with an idealized Gibbs reactor and hence it shows minimum destruction. From the gas turbine there is no exergy loss, as the exhaust stream of the gas turbine is used as the heat source for the block. The exergy analysis reveals, for all the other systems i.e. fuel cell, steam and sCO2 cycle, the loss of exergy to the environment is 30.48%, 43.8% and 63.44% respectively. The exergy loss represents a significant portion of performance degradation, and any improvement measure should be directed to reducing this loss particularly at the tail pipe. For the steam cycle, the tail pipe significant exergetic value suggests another power generation devise can be designed. The integration would increase the performance, but its cost competitiveness should be addressed. In terms of exergy destruction fuel cell system shows improvement potential at the air preheater and the fuel cell stack. The hot stream at the air preheater inlet is at 977.05°C while the cold stream is required to be heated to 770°C. Harnessing the hot stream before the preheater and improving the electrochemical performance of the fuel cell stack can improve the system performance. The steam cycle shows maximum destruction in the turbine owing to low heat source temperature and consequentially low steam generation pressure. For the sCO2 cycle, the low temperature heat source and the recuperator possess considerable potential improvement. With the current boundary conditions and operational parameter, sCO_2 cycle shows maximum power generation and the first law efficiency. However, for a more definitive choice, the optimization of each system by conducting advanced exergy analysis is required and recommended.

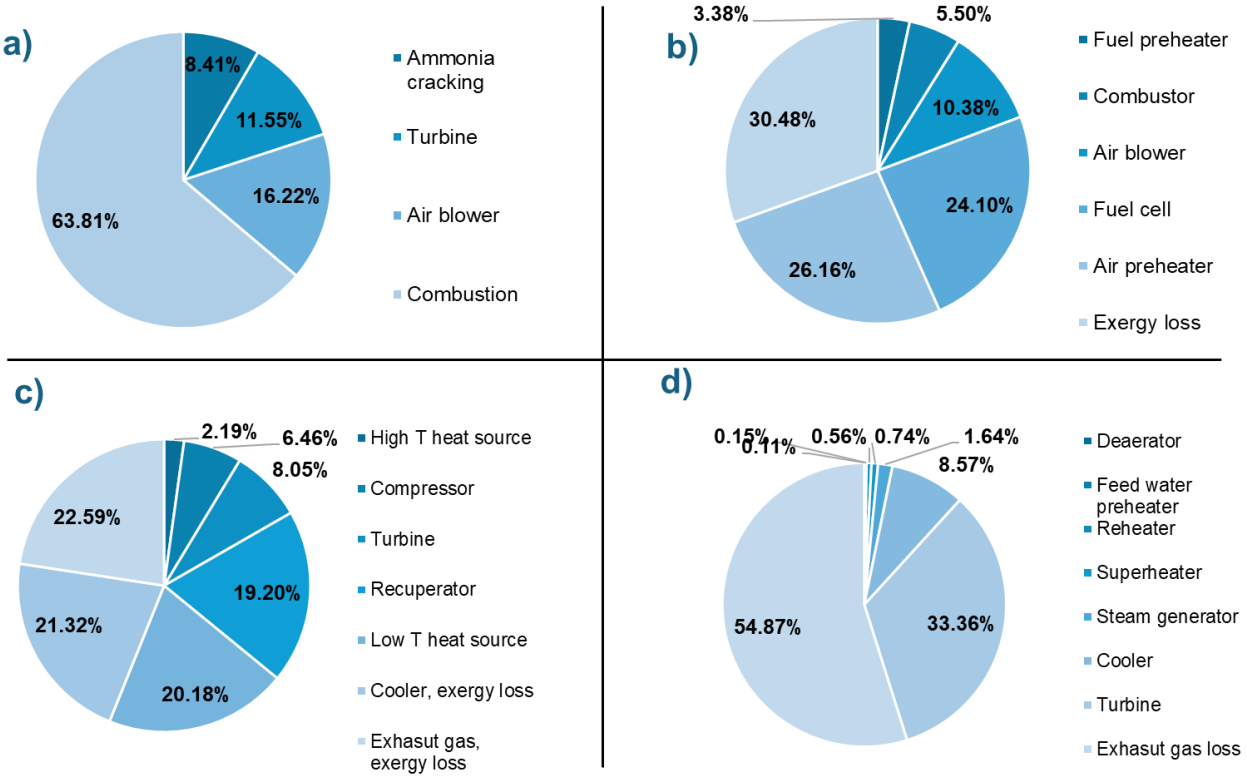

Figure 12. *Exergy destruction ratio of (a) Gas turbine with Ammonia cracking, (b)Fuel cell, (c) sCO2 cycle, and (d) Steam cycle.*

5.3. Limitations and future recommendations

The study selected the M1A-17 turbine by KAWASAKI owing to its 100% H_2 compatibility and operates it with N_2 and H_2 mixture. The current study doesn't incorporate the detailed combustion characteristics; however, the ensuing study is investigating the combustion behaviour with N_2/H_2 or $N_2/ H_2/NH_3$ mixture and evaluating the gas turbine in off-design stage. The impact of separating the N2 from the mixture has also the potential to resolve this limitation and the comparative evaluation of both strategies will be studied. Moreover, the NH_3 cracking was simulated using the Gibbs' reactor, which over-predicts the reactor performance. To rectify this the experimentally corroborated reaction rate is being incorporated in the analysis procedure. In the fuel cell premises, the capacity of couple of MWe. The scale up of fuel cell to MWe class has been done in a straight-line manner by increasing the number of cells. The scaling up of fuel cell requires more detail calculation of number of cells and stacks in one module and the associated balance of plant components which is the subject of a further study. Finally, the exergy analysis reveals the order of destruction in different components, however, the extent of avoidable and unavoidable destruction is a subject of further study.

6. Conclusion

The ammonia as an energy vector has promising potential owing to its high volumetric energy density, established infrastructure and comparatively lower cost with respect to green hydrogen. This study compares characteristics of ammonia as fuel and the representative routes for its electrification with the following key aspects.

- The results showed that the ammonia solid oxide fuel cell can achieve 42% power density in a power compared to hydrogen. The results are promising if the heating value and cost of green hydrogen and ammonia are incorporated.
- The combined-cycle configuration employs a 100% H_2-compatible M1A-17 gas turbine, modified for ammonia utilization by integrating an ammonia-cracking reactor thermally coupled with the turbine exhaust. For the bottoming cycle of the gas turbine, the conventional steam as well as advanced partial heating supercritical carbon dioxide cycle is analyzed to have a thorough comparison.
- The fuel cell system balance of plant was designed to recover the high temperature anode and cathode off gases, and the stack operating temperature was regulated using the air flow and the stack size was calculated to achieve the desired fuel utilization.
- The gas turbine and fuel cell models were validated against experimental and published data to ensure model reliability. The results show that the fuel cell system, steam–gas turbine combined cycle, and supercritical carbon dioxide–gas turbine combined cycle achieve net power outputs of 2.87, 2.65, and 2.90 MW; energy efficiencies of 43.7%, 40.4%, and 44.1%; and exergy efficiencies of 41.0%, 37.9%, and 41.5%, respectively.
- Finally, the second law analysis reveals that a significant portion of exergy 30.48%, 43.8% and 63.44% for fuel cell, steam and sCO2 cycle respectively is lost to the environment, hence, reducing that exergy loss by integrating additional components or varying operational parameter can further improve the system.

Acknowledgments

This study was supported by the Korea Agency of Infrastructure Technology Advancement (KAIA) funded by the Korea government (MOLIT) (Grant number RS-2025-02303377).

References

[1] MacFarlane DR, Cherepanov P V., Choi J, Suryanto BHR, Hodgetts RY, Bakker JM, Ferrero Vallana FM, Simonov AN. A Roadmap to the Ammonia Economy. Joule 2020;4:1186–205. https://doi.org/10.1016/j.joule.2020.04.004.

[2] Valera-Medina A, Xiao H, Owen-Jones M, David WIF, Bowen PJ. Ammonia for power. Prog Energy Combust Sci 2018;69:63–102.

[3] Bird F, Clarke A, Davies P, Surkovic E. Ammonia: zero-carbon fertiliser, fuel and energy store. The Royal Society; Policy Briefing: London, UK 2020:1–40.

[4] Lee B, Winter LR, Lee H, Lim D, Lim H, Elimelech M. Pathways to a Green Ammonia Future. ACS Energy Lett 2022:3032–8. https://doi.org/10.1021/acsenergylett.2c01615.

[5] Ishaq H, Crawford C. Review of ammonia production and utilization: Enabling clean energy transition and net-zero climate targets. Energy Convers Manag 2024;300:117869. https://doi.org/https://doi.org/10.1016/j.enconman.2023.117869.

[6] Tamura M, Gotou T, Ishii H, Riechelmann D. Experimental investigation of ammonia combustion in a bench scale 1.2 MW-thermal pulverised coal firing furnace. Appl Energy 2020;277:115580.

[7] Jeong JH, Kim TS. Integrating ammonia cracking with gas turbine combined cycle for enhanced hydrogen utilization and reduced CO2 emissions. Energy 2025;319:134976. https://doi.org/https://doi.org/10.1016/j.energy.2025.134976.

[8] Cesaro Z, Ives M, Nayak-Luke R, Mason M, Bañares-Alcántara R. Ammonia to power: Forecasting the levelized cost of electricity from green ammonia in large-scale power plants. Appl Energy 2021;282:116009.

[9] Zamfirescu C, Dincer Ijj. Using ammonia as a sustainable fuel. J Power Sources 2008;185:459–65.

[10] Kawasaki Launches World's First 1.8 MW Class, 100% Hydrogen-fueled, Dry-combustion Gas Turbine Cogeneration System 2023.

[11] Ahmad AH, Darmanto PS, Hariana H, Darmawan A, Aziz M, Juangsa FB. Integration ammonia cracking process and co-firing of natural gas in combined cycle power plant: A thermodynamic analysis. Energy 2024;304:132098. https://doi.org/https://doi.org/10.1016/j.energy.2024.132098.

[12] Technologies SESG. EBSILON® Professional for Engineering and Designing Energy and Power Plant Systems 2015.

[13] Muhammad HA, Naseem M, Kim J, Kim S, Choi Y, Lee YD. Solar hydrogen production: Technoeconomic analysis of a concentrated solar-powered high-temperature electrolysis system. Energy 2024;298:131284.

[14] White MT, Bianchi G, Chai L, Tassou SA, Sayma AI. Review of supercritical CO2 technologies and systems for power generation. Appl Therm Eng 2021;185. https://doi.org/10.1016/J.APPLTHERMALENG.2020.116447.

[15] Park SH, Lee YD, Ahn KY. Performance analysis of an SOFC/HCCI engine hybrid system: System simulation and thermo-economic comparison. Int J Hydrogen Energy 2014;39:1799–810.

[16] Lee YD, Ahn KY, Morosuk T, Tsatsaronis G. Exergetic and exergoeconomic evaluation of an SOFC-Engine hybrid power generation system. Energy 2018;145:810–22.

[17] Nanadegani FS, Sunden B. Review of exergy and energy analysis of fuel cells. Int J Hydrogen Energy 2023;48:32875–942.

[18] Muhammad HA, Lee B, Cho J, Rehman Z, Choi B, Cho J, Roh C, Lee G, Imran M, Baik Y-J. Application of advanced exergy analysis for optimizing the design of carbon dioxide pressurization system. Energy 2021;228:120580. https://doi.org/https://doi.org/10.1016/j.energy.2021.120580.